IEEE Access
Multidisciplinary | Rapid Review | Open Access Journal

Received May 3, 2022, accepted May 23, 2022, date of publication June 3, 2022, date of current version June 9, 2022.

Digital Object Identifier 10.1109/ACCESS.2022.3179975

Intelligent Identification Method of Insulator Defects Based on CenterMask

ZHIMING XUAN, JIWEI DING, AND JING MAO
CEEC Jiangsu Electric Power Design Institute Company Ltd., Nanjing 211102, China
Corresponding author: Zhiming Xuan (xuanzhiming@jspdi.com.cn)

ABSTRACT Insulator defect is one of the most important factors for the grid power transmission accidents. However, up till now, traditional insulator defect identification methods cannot meet the requirements of high-speed transmission and high pixel ratio aerial image processing. To solve this problem, in this paper, we proposed a novel method based on CenterMask algorithm to achieve intelligent insulator defect identification. First, the overall architecture of the proposed method that entirely relies on the deep learning models is designed to map the relationship between inputs and outputs. Subsequently, the residual connection and effective Squeeze-Excitation module are introduced to improve the original backbone network, thus overcoming the problem of deep network saturation and channel information loss in the feature layer. Finally, the SAG-Mask with spatial attention mechanism is performed to extract the insulator mask image, while the defect identification and location is realized based on the anchor-free FCOS algorithm. At last, we verify the performance of this proposed method by comparing with other benchmarks, including YOLOv4, SSD and Faster RCNN, which shows high accuracy and good robustness of CenterMask-based insulator defect identification algorithm.

INDEX TERMS Insulator defects, CenterMask algorithm, image processing, insulator mask image.

I. INTRODUCTION

As an essential part of equipment in power transmission systems, electrical insulator is widely used to provide mechanical strength and insulation, which plays a key role in electricity distribution from the power grid to the users. The efficiency of insulators is mainly affected by the conditions of field environment, device pollution, and hardware damage, etc [1]. Occurrence of above situations causes serious problems of varying degrees, especially insulator damage, both to the grid safety and power supply in the whole system. Therefore, the infrastructures require more frequent inspection, repair and maintenance, so as to eliminate malfunctions and insulator defects as much as possible [2]. As a digital engine for the construction and development, intelligent sensing technology effectively satisfies the perception requirements of information depth, breadth, frequency, density and accuracy. Thus, it is more usual to acquire massive on-site pictures of electrical equipment and transmission lines via unmanned aerial vehicles (UAVs) [3] and intelligent robot technology [4], so as to replace manual inspection in harsh working environments [3].

The associate editor coordinating the review of this manuscript and approving it for publication was Andrea F. Abate.

Efficient processing of intelligent perception data is the top priority for the steady promotion and implementation of energy interconnection [5]. The massive intellisense data, including structured, semi-structured and unstructured data, are mainly obtained by monitoring and collecting the status of each part of power generation, transmission, distribution system. These data can be used to evaluate the aging and operation status of essential energy equipment along with its accessories. Defect analysis, defect warning, position of defect areas and components, can be achieved by processing intellisense data with artificial intelligence (AI) algorithms, thus help promote the service efficiency of equipment in all links of the power system [6]. In this way, it can effectively improve the intelligence of control decisions and enhance the operation reliability of the interconnected system.

As one of the key equipment on the transmission side of electric energy subsystem, insulators show the characteristics of large usages, wide varieties and frequent failures. Meanwhile, the operation performance of insulators directly determines the stability and sustainability of the power grid system, as well as other associated energy subsystems. The mature application of aerial photography technology realizes the digitization of insulator defect detection and location [7]. However, due to the large number and size of images taken

by UAVs, more than 5 or even 10 minutes will be cost on image label for each picture in manual, which presents a phenomenon with heavy workload. In addition, the manual process will inevitably lead to miss labeling and error labeling, which further bring security risks on the safe operation of the power grid. Therefore, it is necessary to conduct researches on the intelligent identification of insulator defect by processing and analyzing the massive perception image data [8]–[12].

Up till now, there are dozens of different insulator defect identification methods that have been used and documented. In [13], an online diagnostics method is proposed to detect insulator conditions and predict flashover occurrence. The results show that different target range represent various insulator conditions, thereby promote the accuracy of insulator condition identification and prediction. As detailed in [14], the proposed method is comprised of importing the image with spots, detecting image spots, classifying pattern of each image profile which is applied for each found laser spots pair. Accuracy and recall indices of proposed method can approach 96.101% and 96.317% respectively. Compared with traditional methods, deep learning methods can automatically extract features from images, and shows higher robustness and accuracy [15]–[18]. Reference [19] utilizes the Generative Adversarial Network (GAN) algorithm to achieve insulator defect identification. To further improve the sensitivity of detecting insulator defects, foreground attribute learning and structure attribute learning are incorporated. The precision of benchmarks are all below 0.75, while the proposed method can approach 0.7647. In [20], a Faster R-CNN network is utilized to locate key insulators components. The classification score and anomaly score can be acquired by deep multitask neural network, so as to judge the insulator conditions by analyzing the two scores. The proposed method shows satisfied identification performance compared with other methods. Reference [6] presents a complete system for automatic identification and the diagnosis of electrical insulator strings, which utilizes one fully convolutional network Up-Net as the segmentation component, one convolutional neural network and one Siamese convolutional neural network as the diagnosis component. The accuracy of the proposed method is 99.25%. In [21], low-resolution images are adopted to achieve insulator position detection, thus reduce the time cost and network calculations during computing process. While for fault classification, high-resolution images are used, which help to improve the accuracy of defect classification. The precision, recall, mAP and time values of this proposed method are 94.10%, 92.88%, 93.46%, 231ms respectively. In [22], the Mask RCNN is proposed to extract multiple insulators automatically in the infrared images. Transfer learning, as well as the dynamic learning rate algorithm, are also employed to train the Mask RCNN with the annotated image data.

In summary, the application of deep learning and image processing technology applied in insulator defect identification has become a hotspot in current study. With the widespread popularity of 5G and edge computing technology, the real-time transmission between UAVs and energy equipment inspection data centers will be an inevitable trend. However, most of the existing methods do not take into account the requirements of intelligent perception technology on the efficiency of the insulator defect identification process, which show slightly low performance in the process of defect identification.

To solve this problem, in this paper, we apply a new method, CenterMask, which is proposed in recent years in the computing field as an end-to-end learning based single stage instance segmentation algorithm, to identify the insulator defect among acquired images. It can realize three key tasks, including object feature extraction, mask extraction and self-explosion point detection. Instead of artificially dividing the identification process into multiple subproblems, the novel training model can directly fit the mapping between the original aerial images and the identification results of insulator defect, which effectively avoids the error and time waste caused by the step detection and multi-time segmentation by traditional divide-and-conquer methods. As a result, the CenterMask used method can greatly improve the efficiency and intelligence of the identification process, thus show more important research significance and engineering application value.

The rest of this paper is organized as follows. Section II presents the framework of the proposed intelligent identification method. Section III presents the implementation details. Comprehensive simulation results generated by various benchmarks and proposed method based on real data are reported in Section IV. In Section V, performances of the novel method and benchmarks are presented and concluded, which show the proposed method can significantly improve the accuracy and robustness of identification of insulator defects.

II. FRAMEWORK OF THE PROPOSED METHOD

In usual, the inspection environment of insulator defect identification is generally harsh. Since energy equipment is mostly scattered in the field with dangerous terrain, which may lead to high risk and low efficiency of manual inspection [23]. With the development of technology in recent years, aerial photography and artificial intelligence technology make the inspection process turn from artificial to intelligent, which bring convenience to the grid crews.

In this paper, the inspection efficiency of insulator defect identification and the training complexity of high-quality image identification models are comprehensively considered. As a result, the CenterMask algorithm based mask extraction and self-explosion point detection method is proposed. Based on the one-stage object detection algorithm, the proposed method incorporates the image instance segmentation technology to obtain the mask image of insulators. In addition, the mask extraction of insulator self-explosion point, is also contained in the training process to facilitate the observation of the influence of graph complexity on the effect of

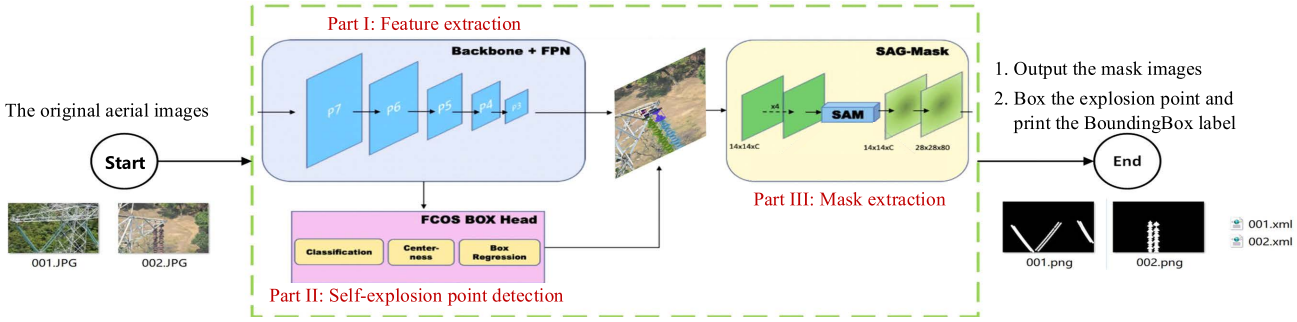

FIGURE 1. The overall framework of the intelligent identification process for insulator defect based on improved CenterMask.

mask extraction. To achieve the insulator defect identification, 4 tasks are further studied in this proposed method, which contain object detection of insulator, mask extraction of insulator, self-explosion point object detection of insulator, and self-explosion point mask extraction of insulator.

According to the above 4 tasks, CenterMask, the anchor-free instance segmentation algorithm based framework is designed. It adopts the improved VoVNet as the backbone network and adds a spatial attention-guided mask (SAG-Mask) module to the fully convolutional one-stage object detection(FCOS) [24]. As illustrated in Fig. 1, the framework mainly includes three parts.

Part I: Feature extraction using backbone network.

Part II: Self-explosion point detection using FCOS.

Part III: Mask extraction using SAG-Mask.

In addition, two optimization ideas are used in the proposed framework to improve the efficiency and accuracy of the identification process. The details are described in Section III.

III. CENTERMASK BASED INTELLIGENT IDENTIFICATION PROCESS FOR INSULATOR DEFECTS

The proposed intelligent identification process of insulator defects aims to satisfy that the intelligent sensing data need to be processed efficiently. Based on the famous one-stage object detection algorithm FCOS, a novel instance segmentation algorithm, namely CenterMask was first proposed by Youngwan Lee and Jongyoul Park in 2019 [25]. Compared with traditional algorithms, it improves the precision and speed of instance segmentation by adding the SAG-Mask module to the FCOS.

A. IMPROVED VOVNET BASED INSULATOR OBJECT FEATURE EXTRACTION

Due to the different angles of aerial photography, the background of insulators in the images shows complexity and diversity, which usually brings serious noise interference to the identification of insulator defects. Therefore, the primary task of insulator defect identification is to ensure the accuracy of object feature extraction, which is realized by backbone network of the model. Dense Block, the core module of the mainstream object detection model DenseNet is shown in Fig. 2. The dense connection of the previous layer will lead to

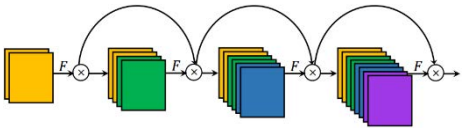

FIGURE 2. The core module of DenseNet. F represents convolution layer and ⊗ indicates concatenation.

a linear increase in the input channel of each subsequent layer, thus resulting in more computation overhead and energy consumption. When handling high-quality aerial images of insulators, the feature extraction process often consumes more video memory and computing time.

The proposal of standard VoVNet effectively overcomes the shortcoming of feature redundancy caused by dense connection. As shown in Fig. 3, it adopts the One-Shot Aggregation (OSA) module by aggregating all features only once in the last feature maps, thus making input size constant and enlarging the new output channel.

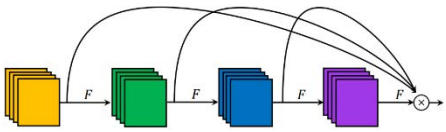

FIGURE 3. Core module of VoVNet.

The backbone network of the CenterMask algorithm utilizes the improved VoVNet(VoVNet-V2), which solves the problems of performance saturation, gradient and information loss in standard VoVNet. Two significant improvements are: 1) Connecting the input to the end of an OSA module, which can backpropagate the gradients of every OSA module in an end-to-end manner on each stage. It enables the training of deeper networks so that can efficiently process the aerial insulator images with a higher pixel ratio. 2) Inspired by the traditional Squeeze-Excitation widely adopted in convolutional neural network (CNN) architectures, an improved channel attention module, namely effective Squeeze-Excitation(eSE), is designed by using only one fully-connected (FC) layer with C channels instead of two FCs without channel dimension reduction. The eSE module is

added to the final layer of the VoVNet to maintain the channel information, thus further enhances the ability of object feature extraction in aerial insulator images.

Fig. 4 shows the connection structure of OSA module in VoVNet-V2, which greatly improves the computing efficiency of graphics processing unit (GPU), thus meet the requirements of intelligent identification and high-speed processing of insulator defects.

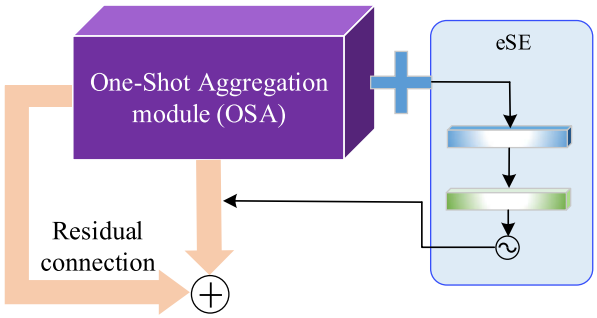

FIGURE 4. The connection structure of OSA module in VoVNet-V2, ⊕ denotes element-wise addition.

B. MASK IMAGE EXTRACTION OF INSULATOR BASED ON SAG-MASK

Reasons such as diverse backgrounds, overlapping insulator images, etc., frequently appear in aerial images, which bring difficulties on insulator defect identification. In addition, the VoVNet-V2 based insulator feature extraction method can merely box the position of the insulator in the original image, whereas cannot achieve accurate image instance segmentation of insulator strings. To solve this problem, CenterMask algorithm achieves this task efficiently by adding the SAG-Mask module to the FCOS.

Compared with the famous instance segmentation algorithm Mask R-CNN and derivation algorithms, or high speed instance segmentation algorithm YOLACT [22], etc., the spatial attention-guided mechanism proposed in Centermask can forecast the mask for each boxed instance by utilizing the spatial attention map of the input image, thus ensuring the high accuracy of the mask extraction.

In this paper, the instance segmentation of insulators is divided into two simple branches. Branch I aims to constrain the local area of each insulator and naturally distinguish the instance, so that a rough shape forecast can be conducted around the center point of each insulator. Branch II aims to accurately segment the insulator image while retaining the spatial position of the segmentation results, thus the salient pixel features of aerial images can be used in the forecasting process. The core idea is to pay attention to the specific block features in the feature map by using the attention mechanism. Finally, the mask image of each insulator is constructed by multiplying the outputs of the two branches. The instance segmentation process of insulators is illustrated in Fig. 5.

The mathematical description of the instance segmentation process in Fig. 5 is: Define the input insulator feature image

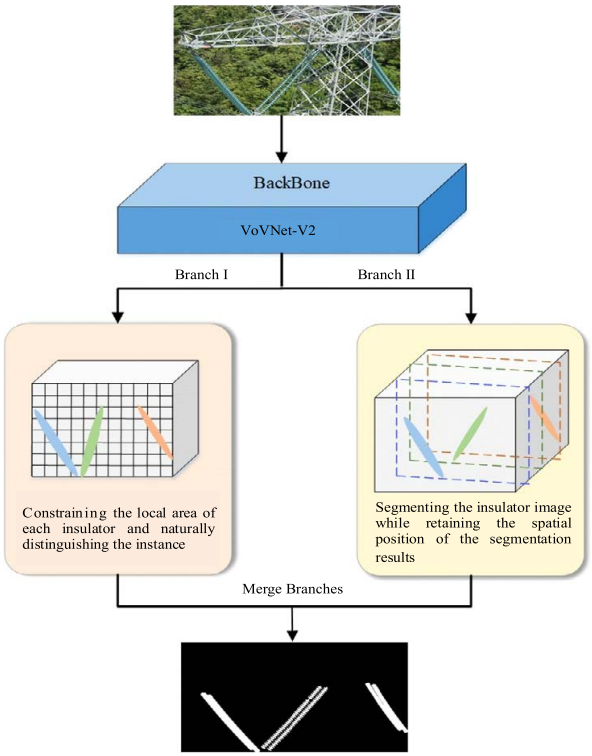

FIGURE 5. The mask extraction flowchart of insulator based on SAG-Mask.

as $X_i \in R^{C*H*W}$, and the features of X_i obtained after max-pooling and average pooling are $P_{\max}, P_{avg} \in R^{1*H*W}$, respectively. Then, P_{max} and P_{avg} are taken as the inputs of a 3×3 convolutional neural network.

$$A_{sag}(X_i) = \sigma(F_{3*x}(P_{\max} \cdot P_{avg})) \tag{1}$$

In branch II, salient pixel features are used to enhance the input features of the original aerial insulator image. By multiplying the original input X_i per-pixel, the mask extraction result X_{sag} can be obtained as follows.

$$X_{sag} = A_{sag}(X_i) \otimes X_i \tag{2}$$

C. LOCATING DEFECTS OF INSULATOR BASED ON FCOS

The aims of insulator defect identification is to intelligently locate various common defects of insulators, such as self-explosion, thick pollution layer and aging cracks, etc. The accurate mask extraction of insulator can merely provide the identification and segmentation of the insulator location in aerial image, while the detection of specific points of the defect needs another trained model. The object detection function of CenterMask is based on the anchor-free FCOS algorithm. It is a fully convolutional one-stage object detection algorithm which realizes the object detection function in the way of per-pixel forecasting. Based on the advantages of the anchor-free process, FCOS avoids the super-parameters setting and the complex calculation related to anchor, thus greatly improving the identification efficiency of insulator defects. The output of this model contains the following three

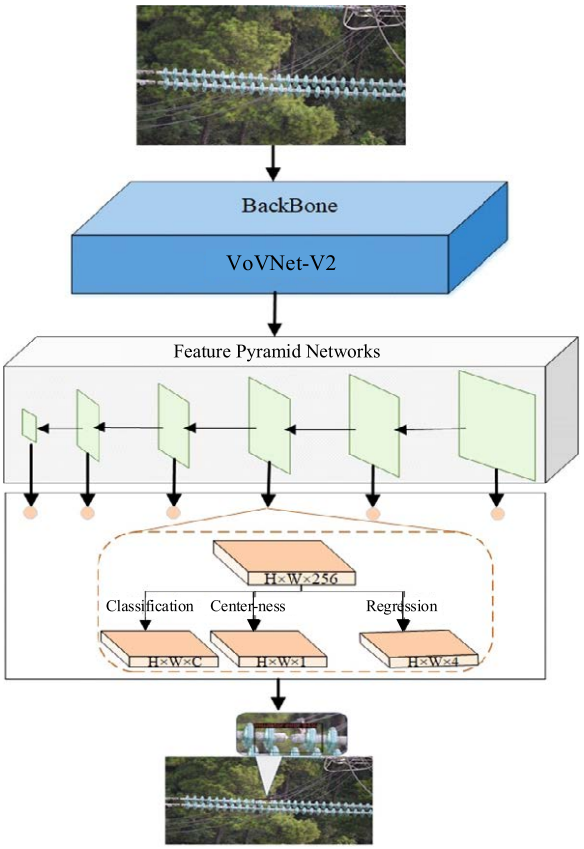

FIGURE 6. The identification flowchart of insulator defects.

parts: regression forecasting pixel by pixel, multiscale feature and Center-ness.

As shown in Fig. 6, the first part of the output is the classification branch. H×W represents the size of the feature image, C represents the number of categories. Any specific coordinate (m, n) in the aerial image can be mapped one by one with the location on the feature image as follows,

$$(\left\lfloor \frac{h}{2} \right\rfloor + m\hat{h}, \left\lfloor \frac{h}{2} \right\rfloor + nh) \tag{3}$$

where h represents the scaling ratio between the feature image and the aerial image.

The second part of the output is the Center-ness strategy. For FCOS algorithm, it not only ensures the high efficiency of anchor-free computation and the high recall of per-pixel regression strategy, but also brings many low-quality forecasting bounding boxes that deviate too much from the center point. This problem can be solved by utilizing Center-ness strategy, which can calculate the distance between each point and the center point, so as to suppress the forecasting bounding boxes far away from the center point. It is worth noting that the Center-ness strategy does not bring in any additional super parameters.

As shown in Fig.6, the Center-ness strategy will add a branch with the classification branch, which is equivalent to adding a loss function to the network. In the process of model training, the forecasting bounding boxes are constrained to be as close to the center as possible through the loss function. As a result, these low quality bounding boxes might be filtered out by the final non-maximum suppression process with high probability. The Center-ness target can be defined as,

$$centerness^* = \sqrt{\frac{\min(l^*, r^*)}{\max(l^*, r^*)} \times \frac{\min(t^*, b^*)}{\max(t^*, b^*)}} \tag{4}$$

$$l^* = m - m_0^{(i)}, t^* = n - n_0^{(i)}$$
$$r^* = m_1^{(i)} - m, b^* = n_1^{(i)} - n \tag{5}$$

where $l*$, $r*$, $t*$ and $b*$ are the distances from the center point to the left, right, top and below sides of the forecasting bounding box, respectively. $centerness*$ represents the value of the loss function.

The third part of the output is the regression branch. The distance to each side of the bounding box is taken as the measurement standard while all points in the box of insulator defect are regressed. It is the main difference between the anchor-free algorithm and the anchor based algorithm.

IV. CASE STUDY

The purpose of this paper is to provide the mask image of insulator strings and the location of defects by training an optimized identification model, so as to replace the traditional high-risk manual inspection efficiently and accurately. The data set of insulator aerial images is provided by a local electric power company in China, which is utilized to evaluate the effectiveness and robustness of the proposed intelligent identification method.

A. EXPERIMENT SETTINGS

Table 1 illustrates the configuration of hardware resources and the software operating environment.

TABLE 1. The experimental environment.

	Type	Configuration
Hardware resource	CPU	Intel(R)Xeon(R)Gold5118 CPU @ 2.30GHz
	GPU	NVIDIA Quadro P5000
	Memory	128G physical memory, 16G video memory
Software environment	sys.platform	win32
	Python	3.7.6 [MSC v.1916 64 bit (AMD64)]
	numpy	1.18.1
	detectron2	0.1.1
	CUDA	10.1
	PyTorch	1.4.0
	GPU 0	Quadro P5000
	Pillow	7.0.0
	torchvision	0.5.0
	cv2	4.2.0

B. INSULATOR MASK IMAGE EXTRACTION

In this section, the collected dataset of insulator aerial images is divided into training set and testing set. Then, sample analysis of training set, selection and optimization of model backbone network, design of training parameters and more than 200,000 times of training are carried out in the above experimental environment. The intelligent identification model of insulator defect is tested on the testing set.

As shown in Fig. 7, the collected dataset should be labeled at the first step since the proposed method is based on the supervised learning algorithm. Fig. 7(a) shows one of the original aerial images. The manual annotation result of Fig. 7(a) using the annotation tool 'Labelme' is shown in Fig.7 (b). The normal insulators are labeled as ''Insulator'' and the insulators with defects are labeled as ''Insulator error''. Then the image annotation is carried out after manual annotation to construct the final model input as can be seen in Fig. 7(c). Finally, the labeled data will be used for training and adjusting parameters of the CenterMask algorithm. Testing set is used to verify the effectiveness of mask extraction branch in the trained CenterMask algorithm. Mask image extraction result is shown as Fig. 8.

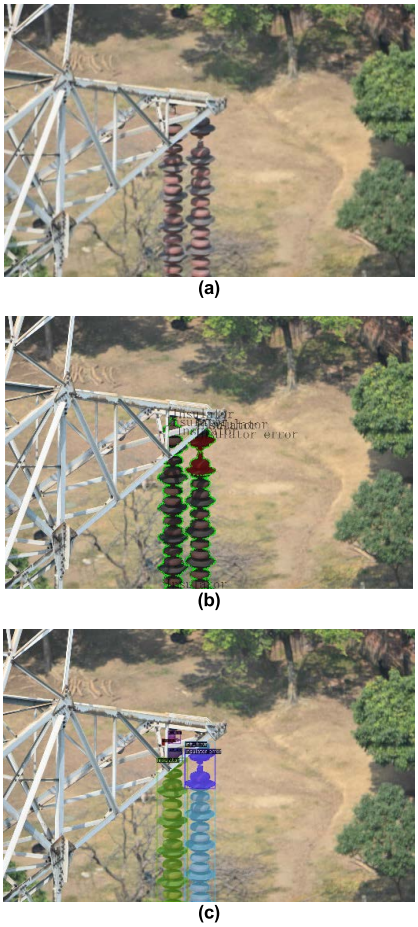

FIGURE 7. Data processing of the aerial images. (a) The original aerial image; (b) The labeled image; (c) The verification image.

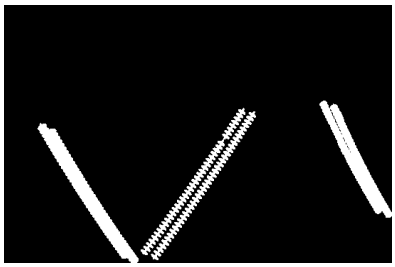

FIGURE 8. Mask image extraction result.

C. INSULATOR DEFECT LOCATING

As illustrated in Section III, the self-explosion point detection branch is independent of the mask extraction branch. In addition, the proposed method makes the input scale expand and shrink randomly within a limited range by setting model parameters, thus enriching the training set.

The proposed method can not only achieve the location identification of self-explosion point in a single image, but also output the XML file storing the location label of self-explosion point. In addition, the identification accuracy will be visually displayed at the same time. Fig. 9 shows the visual output of the identification results and the XML file output on the testing set.

D. CASE INDEX EVALUATION

In this paper, the simulation data are composed with 3 groups of insulator aerial images, which can be identified as insulators in normal condition, insulators in slight defect condition, and insulators in severe defect condition. When there is only one broken area in captured insulator string, the insulator condition can be identified with slight defect; while when the broken area is greater than one place, then the insulator condition can be identified as severe defect. Each test image sequence contains 50 aerial images. In order to verify the practicability and effectiveness of the proposed algorithm in insulator defect identification, we apply 3 benchmarks to make a contrast, such as YOLOv4 [26], SSD and Faster RCNN [27]. To further all-sidedly testify the effectiveness of 4 methods, images with impulsive noise are taken into consideration. Figure 10 shows the identification results in each condition by using all above methods.

From Fig. 10, confidence coefficients of insulator defects are indicated beside red box. As for the normal condition, all methods can figure out correctly, no matter whether there exists pepper noise. As for slight defect condition, confidence coefficient of YOLOv4 is much lower than other 3 methods, while the operating rate is much faster than Fast RCNN and SSD. The reason is that the YOLOv4 algorithm will first apply 1×1 convolution check to achieve dimensionality reduction of feature, and then apply 3×3 convolution kernel to add dimension. During the process of calculation, it enables to greatly reduce the number of parameters

FIGURE 9. Identification and location of insulator defects.

and model size. In the case of severe insulator defects, not all identification methods can figure out the whole defects with high accuracy and speed. There are several missing detection occurring in original methods: YOLOv4, SSD, and Fast RCNN, especially in pepper noise case. Fuzzy images increase the difficulty of insulator defect identification, which reduces the values of evaluation indexes. Nevertheless, the proposed method shows better performance in above cases as shown in Fig. 10.

To further comprehensively and objectively make a contrast between proposed methods and several benchmarks, we apply the following indexes: Average Precision(AP), Average Recall(AR) under different intersection over union(IoU), detected area and number of detections (recorded as AREA and MaxDets, respectively), Frames Per Second(FPS) for comprehensive evaluation. FPS refers to the processed images in one second. The higher the FPS is, the better the algorithm works.

$$AP = \frac{N_{TP}}{N_{TP} + N_{FP}} \tag{6}$$

$$AR = \frac{N_{TP}}{N_{TP} + N_{FN}} \tag{7}$$

Here, N_{TP} means the number of detected insulator defects correctly; N_{FP} means the number of erroneous detected insulator defects; N_{FN} means the number of missing detected insulator defects.

IoU represents the area ratio of intersection to union between the generated candidate box and the original box, which is defined as follows,

$$\text{IoU} = \frac{\text{Area of Overlap}}{\text{Area of Union}} \tag{8}$$

where the value range of IoU is [0,1]. Ideally, IoU is equal to 1.

Detection performances of different models are indicated in Table 1 and Table 2. From the indexes mentioned above, it is not hard to find that the network with improved CenterMask performs better than other existing methods. For example, in insulator severe defect condition, the AP, AR and FPS indexes of proposed method are 2.7%, 3.7%, 6.29 higher than those of the highest corresponding values of other benchmarks by using normal aerial images. For Fast RCNN, for the sake of its low speed, we can draw a simplified conclusion that the requirements of real-time identification of insulator defects is hard to meet. Compared with Fast RCNN, other benchmarks show better effectiveness on processing time.

Except for the characteristics of various networks, some other factors will also affect the identification accuracy. When the captured images are oversize, the resolution of images will be low, in this case, it may evoke identification accuracy reduction and wasted time. What's more, when the background is complex, for instance, the input image is full of transmission line towers and natural scenes, especially the color of natural scenes is similar to the insulators', it will also bring difficulties to the identification and inspection. In the electric power system, most of the string dropping defects are caused by self-explosion of insulators. In the case of detecting slight string-dropping defects of insulators, various algorithms can accurately identify the string-dropping areas of insulators in different extent. However, due to different viewing angles and flying positions of UAVs, there is a high probability that string-dropping areas of insulators are blocked, thus generating missing detection phenomenon. Also, it is not conducive to the separation of sloping captured insulators, and is more likely bring errors in sliding window.

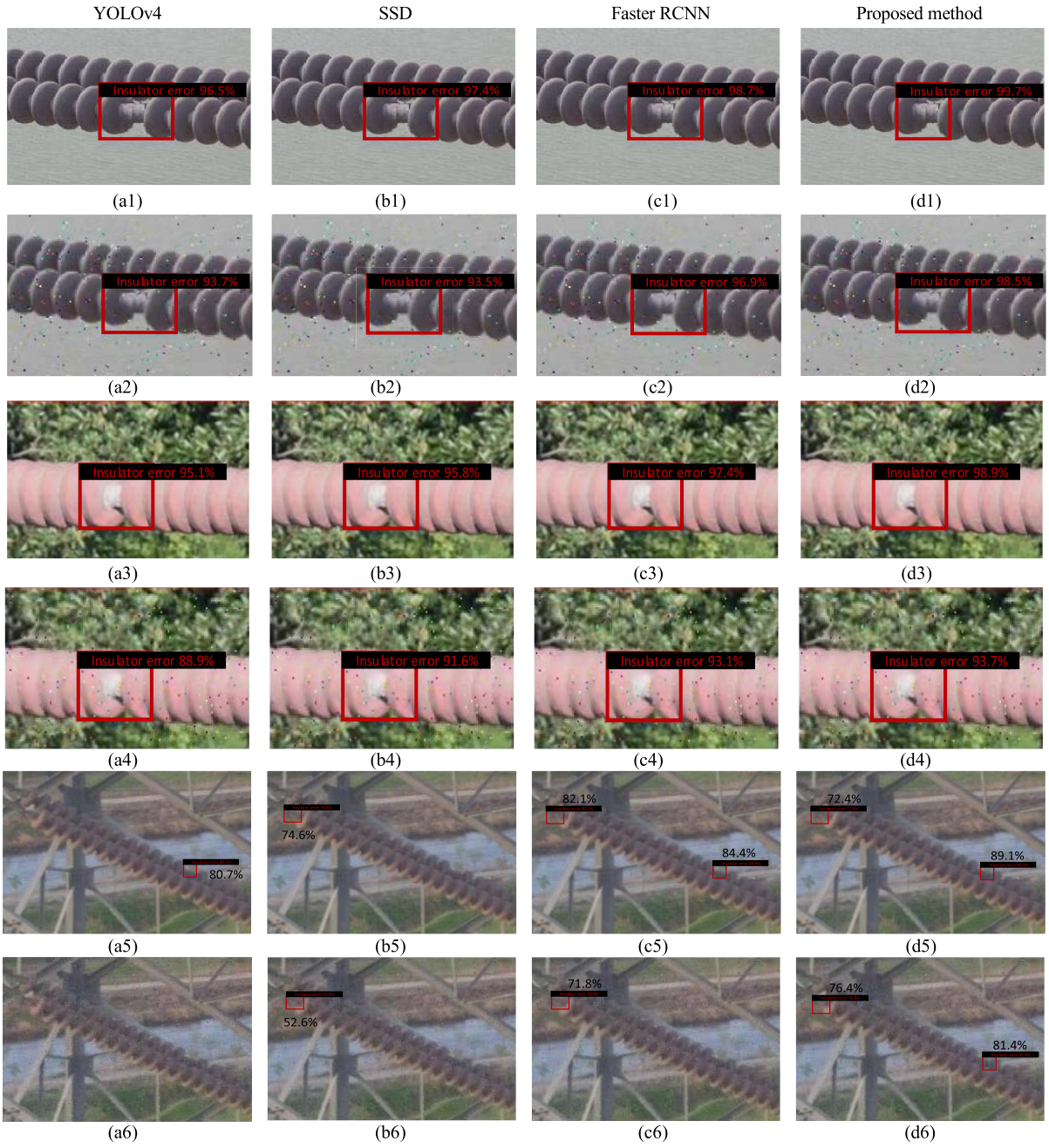

FIGURE 10. Results of insulator defect identification in different conditions by 4 methods.

Besides, exposure effect is also an essential part of accuracy-affecting factors.

To better inquiry the effectiveness of CenterMask-based insulator defect identification method, under the different combinations of metrics which are shown in Table 4, the performance of mask generation and self-explosion point detection are given in Fig. 11 and Fig. 12, respectively. It can be seen that, in Fig.11, when 0.5 is used as the threshold of IoU for instance segmentation, the identification accuracy of insulator defects can fetch up to 94.1%.

The results show that the proposed model can detect most of the obvious self-explosion points of insulators and provide more accurate coordinate information, which can meet the requirements of intelligent identification and high-speed processing of insulator defects.

The proposed method could achieve the best extraction results of insulator mask in aerial images and the AR value could achieve 95.2% when the threshold of IoU and AREA is relatively abundant. The results show that the proposed method can provide accurate and effective instance segmentation of the insulator string. In addition, the processing speed

TABLE 2. Detection performance of different models by using original aerial images.

Method	Insulator condition	Samples	AP	AR	FPS
YOLOv4	Normal	50	100%	100%	22.95
	Slight defect	50	90%	90%	20.74
	Severe defect	50	88.2%	83.3%	19.68
SSD	Normal	50	100%	100%	19.18
	Slight defect	50	93.9%	92%	19.72
	Severe defect	50	90.47%	86.1%	18.84
Fast RCNN	Normal	50	100%	100%	5.99
	Slight defect	50	95.8%	92%	5.47
	Severe defect	50	93.6%	89.8%	5.44
Proposed method	Normal	50	100%	100%	28.15
	Slight defect	50	97.9%	96%	26.68
	Severe defect	50	96.3%	93.5%	25.97

TABLE 3. Detection performance of different models by using aerial images with pepper noise.

Method	Insulator condition	Samples	AP	AR	FPS
YOLOv4	Normal	50	100%	100%	22.62
	Slight defect	50	87.8%	86%	21.37
	Severe defect	50	85.7%	81.4%	20.42
SSD	Normal	50	100%	100%	19.76
	Slight defect	50	88%	88%	19.18
	Severe defect	50	88.4%	85.2%	19.15
Fast RCNN	Normal	50	100%	100%	6.09
	Slight defect	50	93.8%	92%	5.86
	Severe defect	50	91.2%	88.0%	6.04
Proposed method	Normal	50	100%	100%	27.37
	Slight defect	50	95.9%	94%	27.61
	Severe defect	50	94.2%	91.7%	26.05

TABLE 4. Combination of different evaluation metrics.

Metrics	IoU	AREA	MaxDets
AP	0.50-0.95	all	100
AP_{50}	>0.50	all	100
AP_{75}	>0.75	all	100
AP_s	0.50-0.95	small	100
AP_m	0.50-0.95	medium	100
AP_l	0.50-0.95	large	100
AR_{m1}	0.50-0.95	all	1
AR_{m10}	0.50-0.95	all	10
AR_{m100}	0.50-0.95	all	100
AR_s	0.50-0.95	small	100
AR_m	0.50-0.95	medium	100
ARl	0.50-0.95	large	100

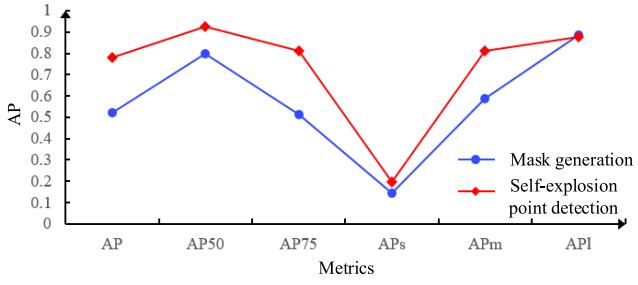

FIGURE 11. The AP curve under different metrics.

and algorithm network improvement will be further investigated as a future work.

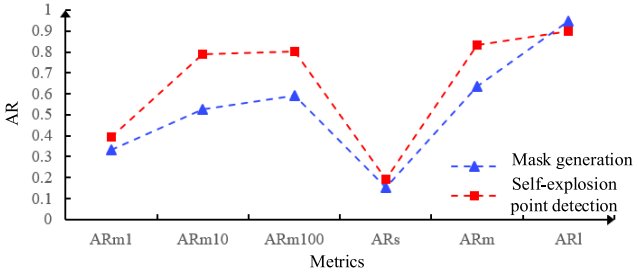

FIGURE 12. The AR curve under different metrics.

V. CONCLUSION

In this paper, the CenterMask-based intelligent identification method of insulator defects is proposed to meet the need of intelligent perception technology on the identification efficiency. In order to overcome the error accumulation of multiple links in the conventional phased and step-by-step insulator defect identification method, the proposed end-to-end learning based one-stage object detection method CenterMask can simultaneously achieve the three key tasks of object feature extraction, mask extraction and self-explosion point detection. The actual aerial images and noise-processed images of insulators are used to verify the effectiveness and robustness of proposed method. In the end, simulations are provided, the comprehensive performance of the proposed method is verified to be better than YOLOv4, SSD, Fast RCNN in AR, AP and FPS. It significantly prevents the waste

of human resources and reduces the potential safety hazards to personnel and power grid operation, thus promoting the continuous development of intelligent inspection of overhead transmission and distribution network in the power system.

REFERENCES

[1] E. Rahman, Y. Zhang, S. Ahmad, H. Ahmad, and S. Jobaer, "Autonomous vision-based primary distribution systems porcelain insulators inspection using UAVs," *Sensors*, vol. 21, no. 3, p. 974, 2021.

[2] W. Godoi, K. Geus, R. Silva, and V. Filho, "Automated flaw detection in X-ray tomography of polymer insulators," *Insight*, vol. 52, no. 10, pp. 533–539, 2010.

[3] T. He, Y. Zeng, and Z. Hu, "Research of multi-rotor UAVs detailed autonomous inspection technology of transmission lines based on route planning," *IEEE Access*, vol. 7, pp. 114955–114965, 2019.

[4] A. Tarik Zengin, G. Erdemir, T. Cetin Akinci, and S. Seker, "Measurement of power line sagging using sensor data of a power line inspection robot," *IEEE Access*, vol. 8, pp. 99198–99204, 2020.

[5] R. Fu, F. Gao, R. Zeng, J. Hu, Y. Luo, and L. Qu, "Big data and cloud computing platform for energy internet," in *Proc. China Int. Electr. Energy Conf. (CIEEC)*, Oct. 2017, pp. 681–686.

[6] C. Sampedro, J. Rodriguez-Vazquez, A. Rodriguez-Ramos, A. Carrio, and P. Campoy, "Deep learning-based system for automatic recognition and diagnosis of electrical insulator strings," *IEEE Access*, vol. 7, pp. 101283–101308, 2019.

[7] D. Sadykova, D. Pernebayeva, M. Bagheri, and A. James, "IN-YOLO: Real-time detection of outdoor high voltage insulators using UAV imaging," *IEEE Trans. Power Del.*, vol. 35, no. 3, pp. 1599–1601, Jun. 2020.

[8] H. Zhang, Z. Hu, Z. Xu, and Y. Song, "Evaluation of achievable vehicle-to-grid capacity using aggregate PEV model," *IEEE Trans. Power Syst.*, vol. 32, no. 1, pp. 784–794, Jan. 2017.

[9] Y. Chi, Z. Liu, X. Wang, Y. Zhang, and F. Wei, "Provincial CO_2 emission measurement and analysis of the construction industry under China's carbon neutrality target," *Sustainability*, vol. 13, no. 4, p. 1876, 2021.

[10] L. Cheng, T. Yu, H. Jiang, S. Shi, Z. Tan, and Z. Zhang, "Energy internet access equipment integrating cyber-physical systems: Concepts, key technologies, system development, and application prospects," *IEEE Access*, vol. 7, pp. 23127–23148, 2019.

[11] J. P. Shang, C. X. Li, and L. Chen, "Location and detection for self-explode insulator based on vision," *J. Electron. Meas. Instrum.*, vol. 31, no. 6, pp. 844–849, Jun. 2017.

[12] Y. Zhai, R. U. I. Chen, Q. Yang, X. Li, and Z. Zhao, "Insulator defect detection based on spatial morphological features of aerial images," *IEEE Access*, vol. 6, pp. 35316–35326, 2018.

[13] M. Palangar and M. Mirzaie, "Detection of critical conditions in ceramic insulators based on harmonic analysis of leakage current," *Electr. Power Compon. Syst.*, vol. 44, no. 16, pp. 1854–1864, 2016.

[14] M. Tomaszewski, P. Michalski, B. Ruszczak, and S. Zator, "Detection of power line insulators on digital images with the use of laser spots," *IET Image Process.*, vol. 13, no. 12, pp. 2358–2366, 2019.

[15] Z. Pu, Y. Xiong, H. Wang, B. Yan, and T. Wu, "Design and construction of a new insulator detection robot for application in 500 kV strings electric field analysis and field testing," *Electr. Power Syst. Res.*, vol. 173, pp. 48–55, 2019.

[16] S. Chandrasekar, C. Kalaivanan, G. C. Montanari, and A. Cavallini, "Partial discharge detection as a tool to infer pollution severity of polymeric insulators," *IEEE Trans. Dielectr. Electr. Insul.*, vol. 17, no. 1, pp. 181–188, Feb. 2010.

[17] M. Bengtsson, R. Gronlund, M. Lundqvist, A. Larsson, S. Kroll, and S. Svanberg, "Remote laser-induced breakdown spectroscopy for the detection and removal of salt on metal and polymeric surfaces," *Appl. Spectrosc.*, vol. 60, no. 10, pp. 1188–1191, 2006.

[18] T. Jabid and M. Uddin, "Rotation invariant power line insulator detection using local directional pattern and support vector machine," in *Proc. Int. Conf. Innov. Sci., Eng. Technol. (ICISET)*, Oct. 2016, pp. 1–4.

[19] B. Ge, C. Hou, Y. Liu, Z. Wang, and R. Wu, "Anomaly detection of power line insulator from aerial imagery with attribute self-supervised learning," *Int. J. Remote Sens.*, vol. 42, no. 23, pp. 8819–8839, 2021.

[20] G. Kang, S. Gao, L. Yu, and D. Zhang, "Deep architecture for high-speed railway insulator surface defect detection: Denoising autoencoder with multitask learning," *IEEE Trans. Instrum. Meas.*, vol. 68, no. 8, pp. 2679–2690, Aug. 2019.

[21] Z. Wang, X. Liu, H. Peng, L. Zheng, J. Gao, and Y. Bao, "Railway insulator detection based on adaptive cascaded convolutional neural network," *IEEE Access*, vol. 9, pp. 115676–115686, 2021.

[22] B. Wang, M. Dong, M. Ren, Z. Wu, C. Guo, T. Zhuang, O. Pischler, and J. Xie, "Automatic defect diagnosis of infrared insulator images based on image instance segmentation and temperature analysis," *IEEE Trans. Instrum. Meas.*, vol. 69, no. 8, pp. 5345–5355, 2020.

[23] Y. Wang, Z. Li, X. Yang, N. Luo, Y. Zhao, and G. Zhou, "Insulator defect recognition based on faster R-CNN," in *Proc. Int. Conf. Comput., Inf. Telecommun. Syst. (CITS)*, Oct. 2020, pp. 1–4.

[24] Z. Tian, C. Shen, H. Chen, and T. He, "FCOS: Fully convolutional one-stage object detection," in *Proc. IEEE/CVF Int. Conf. Comput. Vis. (ICCV)*, Nov. 2019, pp. 9626–9635.

[25] Y. Lee and J. Park, "CenterMask: Real-time anchor-free instance segmentation," in *Proc. IEEE/CVF Conf. Comput. Vis. Pattern Recognit. (CVPR)*, Jun. 2020, pp. 13906–13915.

[26] A. Bochkovskiy, C. Wang, and H. Liao, "YOLOv4: Optimal speed and accuracy of object detection," in *Proc. IEEE Conf. Comput. Vis. Pattern Recognit. (CVPR)*, Apr. 2020, pp. 1–17.

[27] S. Ren, K. He, R. Girshick, and J. Sun, "Faster R-CNN: Towards real-time object detection with region proposal networks," in *Proc. Adv. Neural Inf. Process. Syst.*, 2015, pp. 91–99.

ZHIMING XUAN was born in Jilin, China, in 1995. She received the master's degree in electrical engineering from North China Electric Power University, Baoding, China, in 2021. She is currently working at CEEC Jiangsu Electric Power Design Institute Company Ltd., Nanjing, China. Her research interests include new energy power forecast, relay protection design, and electric transmission design.

JIWEI DING received the B.S. and M.S. degrees in electric engineering from Southeast University, Nanjing, China, in 2013 and 2016, respectively. He is currently working as an Engineer with CEEC Jiangsu Electric Power Design Institute Company Ltd., Nanjing. His research interests include power system relay protection, dispatch automation in power systems, and electric secondary systems.

JING MAO received the M.S. degree in electrical engineering from Hehai University, Nanjing, China, in 2017. She is currently working at CEEC Jiangsu Electric Power Design Institute Company Ltd., Nanjing. Her research interests include power system analysis and new energy accommodation.